tvst

Article

Femtosecond Laser Trabeculotomy in Perfused Human Cadaver Anterior Segments: A Novel, Noninvasive Approach to Glaucoma Treatment

Eric R. Mikula[1,3], Ferenc Raksi[3], Iqbal Ike Ahmed[4,5], Manu Sharma[3], Guy Holland[3], Reza Khazaeinezhad[3], Samantha Bradford[1], James V. Jester[1,2], and Tibor Juhasz[1–3]

[1] Department of Ophthalmology, University of California, Irvine, Irvine, CA, USA
[2] Department of Biomedical Engineering, University of California, Irvine, Irvine, CA, USA
[3] ViaLase Inc., Aliso Viejo, CA, USA
[4] University of Toronto, Toronto, ON, Canada
[5] University of Utah, Salt Lake City, UT, USA

Correspondence: Eric Mikula, Department of Ophthalmology, University of California, Irvine, 843 Health Sciences Road, Irvine, CA 92697, USA.
e-mail: emikula@uci.edu

Received: October 8, 2021
Accepted: February 14, 2022
Published: March 25, 2022

Keywords: femtosecond laser; trabeculotomy; glaucoma; Schlemm's canal

Citation: Mikula ER, Raksi F, Ahmed II, Sharma M, Holland G, Khazaeinezhad R, Bradford S, Jester JV, Juhasz T. Femtosecond laser trabeculotomy in perfused human cadaver anterior segments: A novel, noninvasive approach to glaucoma treatment. Transl Vis Sci Technol. 2022;11(3):28, https://doi.org/10.1167/tvst.11.3.28

Purpose: The purpose of this study was to investigate femtosecond laser trabeculotomy (FLT) in a clinically relevant manner (i.e., delivering the surgical laser beam through the cornea of the intact, human anterior segment to create channels from the anterior chamber into the Schlemm's canal) and to investigate the effect of this treatment on intraocular pressure in perfused human anterior segments.

Methods: Perfused human anterior segments (15 eyes) received either FLT treatment (n = 8) or a sham-treatment (n = 7). Intraocular pressure (IOP) in the perfused samples was recorded before and after treatment. Spectral domain optical coherence tomography, second harmonic generation imaging, and transmission electron microscopy were used to investigate the FLT channels.

Results: The FLT group (n = 7, 1 eye excluded) had a statistically significant reduction in mean IOP of 20.2% from baseline after treatment (5.06 ± 1.46 mm Hg to 4.04 ± 1.63 mm Hg; $P < 0.0005$), whereas the control group (n = 7) remained statistically unchanged (7.72 ± 3.45 mm Hg to 7.78 ± 3.51 mm Hg; $P < 0.71$). Imaging confirmed that the channels traversed the entire trabecular meshwork into the Schlemm's canal.

Conclusions: This study has provided the first direct evidence supporting the feasibility of clinically applicable, noninvasive femtosecond laser trabeculotomy for the treatment of glaucoma. Various imaging modalities revealed minimal collateral damage to adjacent issues.

Translational Relevance: This work demonstrates noninvasive femtosecond laser trabeculotomy in a laboratory setting that is clinically relevant.

Introduction

The only proven treatment for glaucoma is reducing the intraocular pressure (IOP), thus relieving pressure on the optic nerve head lead. This in turn reduces or ideally stops retinal ganglion cell death and progressive visual field loss.[1] The typical treatment paradigm begins with medicated eyedrops, selective laser trabeculoplasty (SLT), then microinvasive glaucoma surgeries (MIGS) before advancing to more traditional filtration surgeries.[2] Each of these treatment modalities comes with its own limitations, ranging from suboptimal patient compliance with eyedrops,[3] limited longevity with SLT,[4,5] an ab interno approach requiring a corneal incision with MIGS,[6] to the invasive and complex nature of traditional filtration surgeries and the risks and difficulties associated with their postoperative management regimens.[7,8]

After eyedrops SLT is the next treatment in the hierarchy of treatment escalation. SLT uses a laser that is selectively absorbed by the pigmented

endothelial cells of the trabecular meshwork (TM), causing thermal damage to the cells and resulting in a cascade of biological effects thought to increase hydraulic conductivity of the inner wall of the Schlemm's canal.[9,10] Subsequently, MIGS are typically the next treatment because of their minimally invasive nature and favorable safety profiles. In fact, MIGS are increasingly viewed as an alternative to medical therapy as opposed to being seen as an alternative to filtering surgery.[11] MIGS procedures target three anatomical categories, namely the Schlemm's canal, suprachoroidal space, or subconjunctival space.[6] The majority of MIGS, however, target the Schlemm's canal and operate on the principle of reducing or bypassing the resistance to aqueous humor outflow encountered in the TM, juxtacanalicular tissue, and inner wall of the Schlemm's canal. Once this resistance is removed, the aqueous can directly pass into collector channels, aqueous veins, and eventually into the episcleral venous system. For example, implants such as the iStent (Glaukos Corporation, San Clemente, CA, USA) and Hydrus Microstent (Ivantis, Inc., Irvine, CA, USA) bypass the resistance in the TM via a small tube-like implant through the TM and into the Schlemm's canal.[12,13] Other devices, such as the Trabectome (NeoMedix, Irvine, Ca)[14] and Kahook dual blade (New World Medical, Rancho Cucamonga, CA, USA),[15] physically remove the TM by electrocautery or mechanical cutting, respectively. Excimer laser trabeculostomy (ELT) is a laser-based MIGS procedure that creates holes through the TM into the Schlemm's canal via nonthermal absorption of ultraviolet laser light and ionization of the TM. Published data report the longevity of this procedure and patency of the holes out to at least two years, although the eye must still be opened to introduce the laser.[16,17]

Most MIGS procedures, ELT included, bypass the traditional outflow pathway by introducing direct aqueous humor communication between the anterior chamber and Schlemm's canal. However, these transtrabecular procedures require a corneal incision and the introduction of varying degrees of instrumentation into the anterior chamber. As such, there is an unmet medical need for a glaucoma treatment that can bypass the aqueous humor outflow resistance found in the TM region without the need to open the eye. To this end we developed a novel device, the ViaLase laser system, (ViaLase, Inc. Aliso Viejo, CA, USA), which delivers tightly focused femtosecond laser pulses through the cornea and across the anterior chamber to the iridocorneal angle, thus creating channels through the trabecular meshwork and into the Schlemm's canal. We have previously demonstrated that femtosecond laser channels created directly through the TM (not delivered through the cornea) in a nonclinically relevant manner can lower IOP in perfused human anterior segments.[18] The objective of this study was to investigate the efficacy of femtosecond laser trabeculotomy (FLT) in a clinically relevant manner (i.e., by focusing through the intact cornea to deliver FS laser pulses to the TM using the ViaLase, Inc., laser system).

Methods

This study used a custom femtosecond laser system designed and built by ViaLase, Inc., to perform femtosecond laser trabeculotomy on perfused corneoscleral shells (anterior segments). The effect of the procedure on IOP in the perfused anterior segments was measured. Sample tissues were imaged using second harmonic generation microscopy (SHG), optical coherence tomography (OCT), and transmission electron microscopy (TEM). This study was determined not a be a human subject study and was performed in compliance with the principles of the Declaration of Helsinki.

Surgical Device

The laser delivery system was designed and built by ViaLase, Inc., to deliver tightly focused femtosecond laser pulses through the intact cornea, across the anterior chamber, and to the outflow structures (trabecular meshwork, juxtacanalicular tissue, and Schlemm's canal) via custom delivery optics. A regeneratively amplified femtosecond laser producing 400 femtosecond (fs) pulses at 1030 nanometers was used as the laser engine (NKT Photonics, Birkerød, Denmark). The laser was aligned into a custom delivery system comprising laser scanning mirrors, a camera, an aiming laser, an objective lens, and finally custom eye tissue interface optics that couple light into the iridocorneal angle. The spot size out of the delivery system was measured to be less than 10 µm. The scanning mirrors and objective lens were controlled using custom ViaLase, Inc., software capable of scanning the focal point of the femtosecond laser in a contiguous rectangular volume along the axis of the laser. A 632.8 nm HeNe aiming laser (Thorlabs, Inc., Newton, NJ, USA) was split into two parallel beams and coaligned with the femtosecond beam through the delivery system. The aiming beams overlapped into a single spot at the focal point of the system, thus indicating the focal point of the infrared treatment laser.

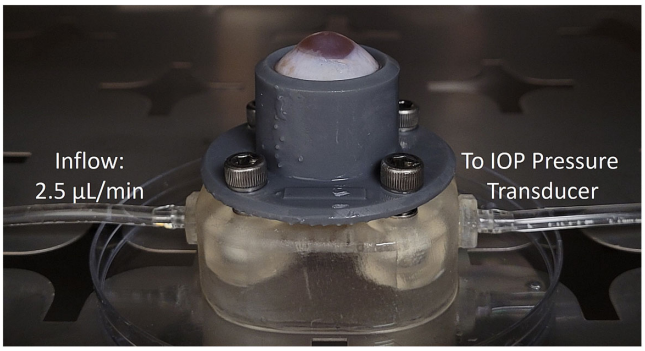

Figure 1. Corneoscleral shell mounted to the perfusion device.

Human Anterior Segment Perfusion Model

Constant flow, variable pressure anterior segment perfusion has previously been used by our group and others to evaluate the effect of interventions on IOP and is described in detail elsewhere.[18–22] Measuring IOP (mm Hg) was chosen instead of outflow facility (µL/min/mm Hg) because of the clinical relevance of IOP. Briefly, 15 dissected corneoscleral shells with no known history of glaucoma, ocular hypertension, or trabecular meshwork procedures and an average age of 70.4 ± 5.6 years were received within 24 hours of death from the San Diego Eye Bank and preserved in Optisol GS corneal transplant media (Chiron Intraoptics, Irvine, CA, USA). The posterior segment, vitreous, lens, iris, and choroid were removed. The tissues were mounted to a custom artificial anterior chamber and perfused in a tissue culture incubator at 37°C, 5% CO_2, and 95% humidity (Sheldon Manufacturing Inc, Cornelius, OR, USA). Figure 1 shows a corneoscleral shell mounted to a custom artificial anterior chamber perfusion device. The inflow rate of perfusion media (Dulbecco's modified Eagle media supplemented with 100 U/mL penicillin, 100 µg/mL streptomycin, 5 µg/mL amphotericin B) was set to the physiological inflow rate of 2.5 µL/min via a syringe pump (PHD 2000; Harvard Apparatus, Inc., Holliston, MA, USA), while the pressure within the anterior segment was recorded via a computer-controlled pressure transducer at one-minute intervals (PX409-GUSBH; Omega Engineering, Norwalk, CT, USA). Each anterior segment was perfused for at least 12 hours before treatment to achieve a baseline IOP. After FLT or sham-treatment, perfusion was recontinued for an additional 12 hours to obtain postprocedure IOP before the experiment was terminated.

Gonioscopic FLT and Sham Treatment

Eight anterior segments received FLT (treatment group), whereas seven anterior segments received the sham treatment (control group). During FLT treatment the anterior segment, while mounted to the artificial anterior chamber, was removed from the incubator and coupled to the surgical device via a custom corneal interface optic using GenTeal Gel (Novartis, Basel, Switzerland). First, the trabecular meshwork was identified using the gonioscopic camera; next the computer-controlled scanning mirrors and objective lens were adjusted to overlap the dual aiming beams onto the surface of the trabecular meshwork, thus ensuring that the surgical laser was also focused onto the TM at the desired location. The lower uveoscleral meshwork was targeted because the Schlemm's canal is anatomically distal to this region. A typical view of the trabecular meshwork and overlapping aiming beams in the perfused anterior segment is presented in Figure 2.

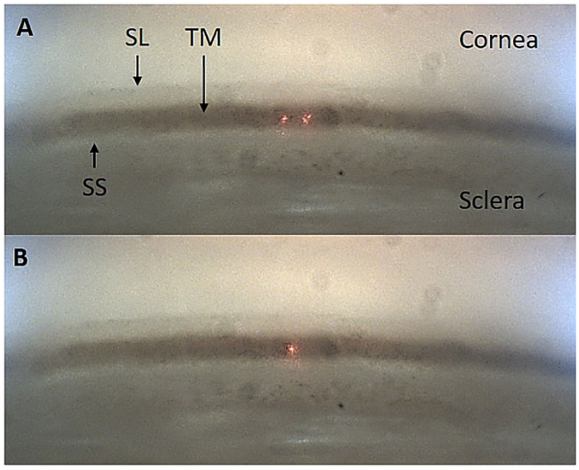

Figure 2. A typical ViaLase Inc. gonioscopic image acquired through an intact ex vivo perfused human anterior segment. The cornea, sclera, Schwalbe's line (SL), trabecular meshwork (TM), and scleral spur (SS) are clearly visible. The iris has been excised. (A) The dual aiming beams on the TM. (B) The dual aiming beams overlapped to a single point on the TM, indicating the focal plane of the femtosecond laser.

Each sample in the FLT treatment group received three channels measuring 500 µm wide, by 200 µm high, through the full thickness of the TM. Each channel accounts for less than 5° of the iridocorneal angle. Figure 3 shows the laser scan pattern overlayed on the iridocorneal angle outflow structures. The pulse energy and repetition rate of the laser were 14 µJ and 10 kHz, resulting in an average power of 140 mW. The length of pattern along the axis of the laser was longer than the orthogonal thickness of the TM because of the oblique angle of incidence of the surgical laser relative to the tissue. The control eyes underwent the same procedure with the exception that the femtosecond laser was not turned on; therefore no channels were created.

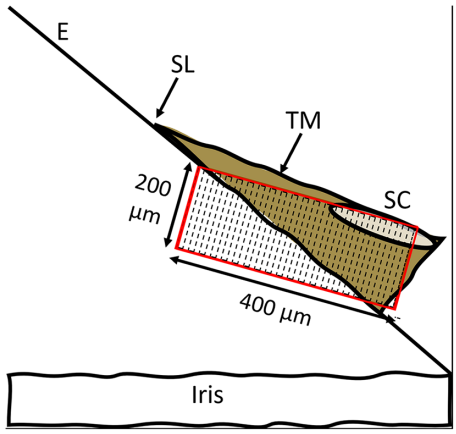

Figure 3. The laser scan pattern is 200 µm high, 500 µm wide circumferentially (into the plane of the paper, not shown), and 400 µm long in the depth direction. E, corneal endothelium; SL, Schwalbe's line; TM, trabecular meshwork; SC, Schlemm's canal.

Imaging

FLT channels were imaged to determine whether they fully penetrated the Schlemm's canal and to assess potential collateral damage to adjacent tissues.

OCT

A custom-built spectral domain (SD) OCT was used to confirm that the femtosecond laser drainage channels penetrated the Schlemm's canal through the TM. The SD-OCT had a central wavelength of 850 nm and theoretical axial and lateral resolutions of 2.7 µm and 8.2 µm in air, respectively. Further serial OCT imaging of an FLT channel and a three-dimensional (3D) reconstruction of the channel were performed. To generate the 3D reconstruction of the channel and surrounding tissue, B-scans were acquired at 5-µm intervals along a 1.5-mm distance circumferentially. Three hundred images were cropped and assembled into a TIFF stack in ImageJ before being exported to FluoRender software for 3D reconstruction (Scientific Computing and Imaging Institute, Salt Lake City, UT, USA).

Two-Photon Imaging

Nonlinear or two-photon imaging uses nanojoule femtosecond laser pulses in the near infrared to generate autofluorescent or second harmonic signals in biological tissues. Tissue was fixed in paraformaldehyde and 250 µm thick vibratome sections were cut through the cornea-sclera in the region of the FS channel using a Campden Instruments Ci 5100 M2 Vibratome (Loughborough, England). A multiphoton microscope (Leica SP8 Falcon; Leica, Wetzlar, Germany) was used to perform SHG and two-photon excited fluorescence imaging. SHG and autofluorescence signals were generated using 820 nm FS pulses, and emission spectra were collected from 390 to 430 nm and 450 to 550 nm for SHG and autofluorescence, respectively. Images were taken within the region of the trabeculotomy and in untreated adjacent tissues.

TEM

Tissue samples were fixed in glutaraldehyde and further prepared for TEM by Outermost Technology (Santa Clara, CA, USA). Imaging was performed at the Department of Health Sciences of the University of Utah. The outer wall of Schlemm's canal was imaged in control tissue and adjacent FLT-treated tissue to investigate potential thermal collateral damage adjacent to the laser channel.

Statistics

A two-way repeat measures analysis of variance using SigmaStat (Palo Alto, CA, USA) was performed to determine whether significant differences existed between pretreatment and post-treatment perfusion pressures for each group (FLT and sham) and between the baseline perfusion pressures between both arms (FLT vs. sham).

Results

Perfusion IOP

The FLT group (n = 7, 1 eye excluded) had a statistically significant reduction in mean IOP of 20.2% from baseline following treatment (5.06 ± 1.46 mm Hg to 4.04 ± 1.63 mm Hg; $P < 0.0005$), while the control group (n = 7) remained statistically unchanged (7.72 ± 3.45 mm Hg to 7.78 ± 3.51 mm Hg; $P < 0.71$) after 12 hours. The IOP data for all eyes are presented in the Table. Despite a drop in IOP of 38%, eye number eight in the FLT group was excluded from statistical analysis because the baseline IOP was well outside of the normal physiological range. Although the mean baseline IOP in the control group was higher than the baseline IOP in the FLT group, the difference was not statistically different ($P = 0.11$).

OCT

Figure 4 contains two cross-sectional OCT images showing the untreated tissue (A) (in the vicinity of the femtosecond laser treatment) and the femtosecond laser created drainage channel (B) in a sample eye. Schlemm's canal is visible in Figure 4A along with the TM, Schwalbe's line, and residual iris root left over from tissue dissection. Figure 4B shows the FLT

Table. IOP Data for FLT and Control Groups

	IOP (mm Hg)		
	Before Treatment	After Treatment	ΔIOP (%)
FLT			
1	5.7 ± 0.7	4.4 ± .2	22.9
2	6.1 ± 0.4	5.9 ± 0.2	3.6
3	3.5 ± 0.6	2.3 ± 0.1	35.3
4	6.4 ± 0.5	5.6 ± 0.2	12.6
5	3.8 ± 0.2	2.8 ± 0.1	27.4
6	6.9 ± 0.2	5.7 ± 0.1	17.5
7	3.0 ± 0.2	1.7 ± 0.2	42.3
8*	20.6 ± 1.3	12.6 ± 1.8	38.7
Mean	5.1	4.0	20.0
σ	1.5	1.6	
P	0.0005		
Control			
1	13.1 ± 0.8	12.7 ± 0.4	3.4
2	12.5 ± 0.5	13.2 ± 0.3	−5.4
3	6.2 ± 0.3	6.5 ± 0.3	−4.3
4	4.2 ± 0.4	3.8 ± 0.1	9.6
5	5.5 ± 0.2	5.5 ± 0.3	0.0
6	4.4 ± 0.3	4.6 ± 0.4	−5.2
7	8.1 ± 0.3	8.2 ± 0.3	−1.1
Mean	7.7	7.8	−0.8
σ	3.5	3.5	
P	0.7		

The mean drop in IOP for the FLT group was 20% compared to baseline. Eye no. 8 in the FLT group was excluded from analysis because the baseline IOP was out of physiological range.

channel fully penetrating Schlemm's canal through the full thickness of the trabecular meshwork. Schwalbe's line is intact, and a large collector channel is also visible.

Figure 5 shows a 3D OCT reconstruction of the TM in the region of the FLT channel. The image shows a channel with well-defined edges and shows that this treatment was located above what appears to be a collector channel. Also depicted in the figure is that the channel becomes deeper posteriorly, following the natural wedge-shaped contour of the trabecular meshwork itself. This is due to the oblique angle of the incoming laser relative to the target tissue, as depicted in Figure 3.

Two-Photon/SHG Imaging

Figure 6 is a two-photon autofluorescence (Green)/SHG (Magenta) image showing the intact trabecular meshwork region adjacent to the FLT channel (A, B) as well as the region containing the FLT channel (C, D). Panel A was taken with an objective ×20 and shows the intact TM, Schlemm's canal, and Schwalbe's line. Panel B was taken with a ×63 objective and shows a zoomed image of the Schlemm's canal and juxtacanalicular region. The outer wall is intact and continuous. Panel C was taken with an objective ×20 and shows the FLT drainage channel passing completely through the TM and into Schlemm's canal. Schwalbe's line is undisturbed. Panel D was taken

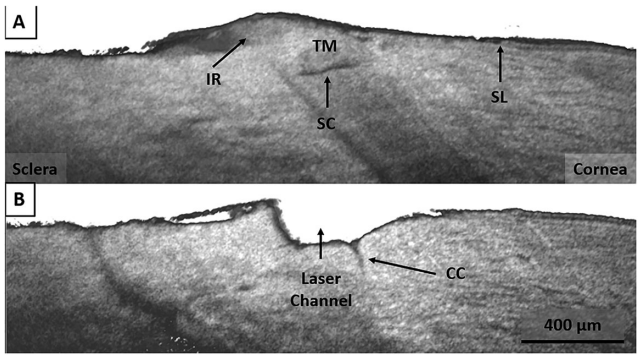

Figure 4. (A) SD-OCT showing the intact TM and Schlemm's canal (SC) in the region adjacent to the FLT drainage channel. Schwalbe's line (SL) and residual iris root (IR) are also visible. (B) SD-OCT showing the FLT channel penetrating Schlemm's canal through the trabecular meshwork. Also visible is a large collector channel within the region of the FLT channel.

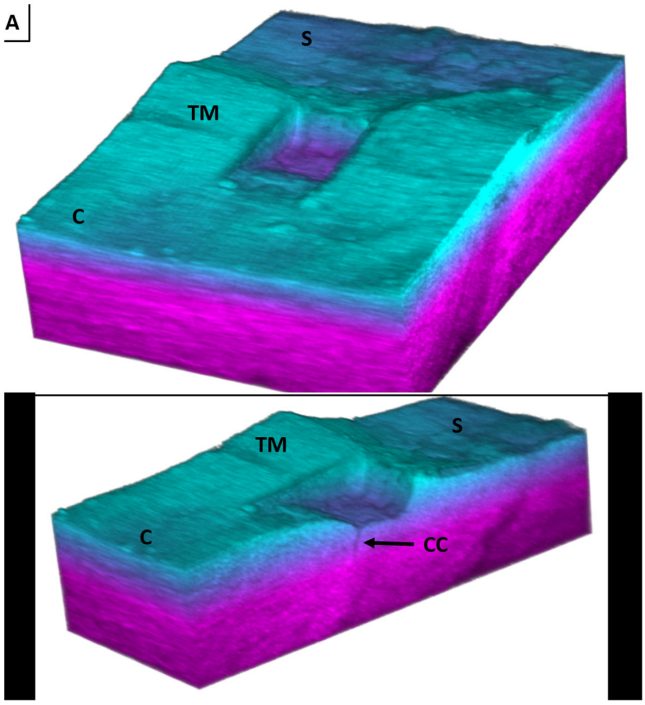

Figure 5. A 3D spectral domain OCT reconstruction of an FLT channel (c-cornea, s-sclera, TM-trabecular meshwork, cc-collector channel). (A) Full image showing the wedge shape and well-defined edges of the FLT channel. (B) Cross-section of the FLT channel showing a collector channel.

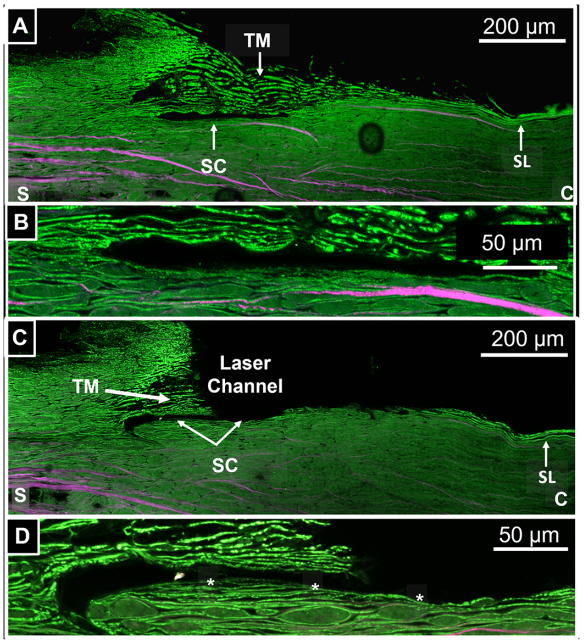

Figure 6. (A) Autofluorescence/SHG image taken with a 20x objective showing the intact TM, Schlemm's canal, and Schwalbe's line (SL). (B) Zoomed in image of SC region from (A) taken with a ×63 objective. (C) Autofluorescence/SHG image taken with a ×20 objective showing the FLT drainage channel, Schlemm's canal (SC), residual TM, and Schwalbe's line (SL). (D) Zoomed in image of the SC region from (C) taken with a ×63 objective. *Asterisks* demarcate undisturbed tissue layer connecting FLT channel region to inner region of SC.

with an objective ×63 and shows a zoomed image of the FLT drainage channel, remaining TM, and outer wall of Schlemm's canal. The asterisks demarcate a continuous layer of tissue on the surface of the outer wall, which begins inside of the Schlemm's canal and continues outward undisturbed into the region of the FLT drainage channel.

TEM

Figure 7 shows TEM images at magnification ×2000 of the outer wall of Schlemm's canal in the untreated TM/SC region (7A) and in the adjacent treated region within the same sample (7B). Panel 7A shows the intact outer wall in an untreated control region. The endothelium is present as are some adjacent structures. About 5 to 10 µm distal to the outer wall endothelium collagen bundles begin to appear, as indicated by stars and arrows. Panel B shows the outer wall of Schlemm's canal in the adjacent FLT treated region. The endothelium and adjacent structures have been removed, although the collagen bundles, as in 7A, are undisturbed.

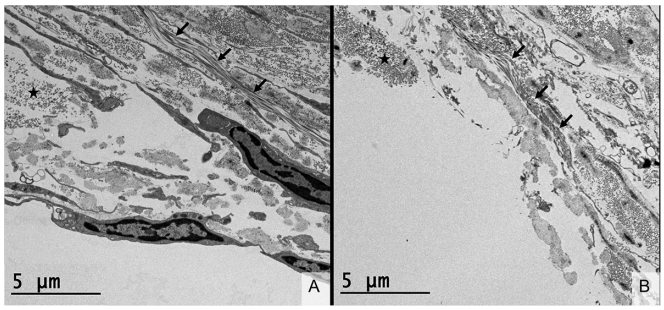

Figure 7. Transmission electron microscopy (TEM, ×2000) of the outer wall of Schlemm's canal in untreated control tissue (A) and tissue treated by femtosecond laser trabeculotomy (B). (A) The endothelium of the outer wall of Schlemm's canal is intact with orthogonal collagen bundles beginning 5 µm beyond the endothelial layer, as demarcated by the *star*. These collagen fibrils are running into the plane of the image. A transverse bundle of collagen is demarcated by *arrows*. (B) The endothelial layer of the outer wall of Schlemm's canal has been removed in this sample. The orthogonal and transverse collagen bundles (*star* and *arrows*, respectively) are present and a similar location relative to Panel A. The collagen fibrils (<100 nm in diameter) are intact adjacent to the FLT treatment area, indicating that there is no thermal collateral damage.

Discussion

The current study introduced a novel technology, the ViaLase, Inc., laser system for glaucoma treatment, capable of delivering tightly focused femtosecond laser pulses through the cornea and into the iridocorneal angle to noninvasively create drainage channels through the TM and into the Schlemm's canal. The channels resulted in a significant reduction in IOP of 20.2% in perfused anterior segments. The Schlemm's canal tends to collapse in some regions of the cadaver eye. For this reason, three channels were created to increases the chances of penetrating a noncollapsed region of Schlemm's canal. Our group previously investigated the effect of femtosecond laser channels created directly through the TM in a cuvette containing a corneoscleral shell with the TM facing upward toward the laser.[18] That study found that FLT channels significantly lowered IOP by 22% in perfused human anterior segments when compared to baseline and control tissues. The current study builds on what was learned previously in that the significant technical challenge of delivering tightly focused femtosecond laser pulses through the cornea and into the iridocorneal angle was overcome. Using custom designed delivery optics, we were able to achieve a spot size small enough for photodisruption in the TM at low pulse energies (14 µJ). As in our previous study,[18] this study showed FLT drainage channels can

reduce IOP in constant inflow perfused human anterior segments by about 20%. This agrees with previous studies investigating trabecular bypass implants, such as the iStent and Hydrus Microstent, which resulted in either IOP reduction or outflow facility increase in the perfused anterior segment of 20% to 70%.[13,22–24] Because much of the aqueous outflow resistance is thought to reside in the juxtacanalicular tissue and inner wall of Schlemm's canal, the circumvention of this tissue is expected to reduce IOP. As in our previous study, it is important to note that baseline IOP values reported in the current study were significantly lower than the average physiological IOP of 15 mm Hg.[25] The lack of episcleral venous back pressure (7–11 mm Hg) in the perfusion model accounts for this discrepancy.[26–28]

Femtosecond lasers have been used previously to photodisrupt the trabecular meshwork in human tissue, primate tissue, and porcine tissue. In human tissues, Toyran et al.[29] directly photodisrupted the TM in excised tissue (without a gonio lens) and were able to penetrate fully through the TM and, with certain combinations of pulse energy and exposure time, penetrated well into the sclera. That study demonstrated that direct irradiation of the human TM with amplified femtosecond pulses (7–14 µJ pulse energies) could penetrate the Schlemm's canal without causing any thermal damage. However, their approach did not use a gonio lens with laser delivery through the intact cornea. Studies in primate and porcine tissue investigated the delivery of amplified femtosecond laser pulses to the TM and iridocorneal angle using a gonio lens (Magna View Gonio Laser Lens; Ocular Instruments, Inc., Bellevue, WA, USA).[30,31] These studies used significantly higher pulse energies (40–240 µJ) but failed to fully penetrate through the TM to the Schlemm's canal. This was likely due to the significant optical aberrations introduced when focusing femtosecond laser pulses through a traditional gonio lens and the cornea at such an oblique angle. Traditional gonio lenses, such as those used during SLT, are designed to achieve spot sizes hundreds of micrometers in diameter and are not suitable for femtosecond photodisruption. Our group previously used amplified femtosecond laser pulses tuned to 1.7 µm to create partial thickness scleral drainage channels for lowering pressure in a live rabbit model.[32] Although the approach showed some promise, the generation of amplified FS pulses at 1.7 µm was cumbersome.

Nonlinear imaging of the outer wall of Schlemm's canal (Fig. 6B) appeared to show an intact collagen bundle a few micrometers in diameter extending from within the Schlemm's canal out to the region of the FLT treatment. The continuity of the fiber in the region of the FLT drainage channel suggests that the FLT treatment did not penetrate the outer wall of the Schlemm's canal. Additionally, there is a loss of the second harmonic signal associated with thermal damage or thermal denaturization of collagen.[33,34] The presence of the fiber itself in the image indicates that there is no thermal damage. Despite this, the resolution of the SHG image was insufficient to determine the true extent of the FLT channel beyond the outer wall, if any at all. TEM presented in Figure 7 showed that the FLT channel did in fact extend slightly past the outer wall of Schlemm's canal by 5 to 10 µm. It is important to note that the collagen bundle and individual fibrils, demarcated by the star in panel 6B, are on the exact border of the FLT channel and remain intact. This finding indicates that there is no thermal collateral damage to the tissue adjacent to the treatment. Although the FLT treatment did extend further than intended by up to 10 µm, it was to be expected because the depth of treatment was adjusted subjectively based on the appearance of the aiming beams on the gonio camera. Further iterations of the ViaLase laser system can potentially incorporate more sophisticated imaging to fine-tune the treatment depth. Such an improvement would ensure that the outer wall of Schlemm's canal would remain untouched. However, it is not uncommon to damage the outer wall of the Schlemm's canal in glaucoma surgeries. Traditional filtering surgeries, such as ab externo trabeculectomy, routinely unroofed the Schlemm's canal, essentially removing a portion of the outer wall manually.[7] Common MIGS procedures such as the Trabectome (NeoMedix, Irvine, CA, USA) and dual-blade goniotomy also result in collateral damage to the outer wall of Schlemm's canal. Kahook et al.[35] presented preclinical histology in human cadaver tissue that had undergone either a Trabectome procedure or dual-blade goniotomy. In both instances there was clear discontinuity and damage in the outer wall on the order of tens of micrometers distal to the Schlemm's canal. Additionally, Yu et al.[36] demonstrated that the outer wall of the Schlemm's canal can be ablated during ELT (~50 µm) in cadaver tissue if the treatment is applied too deeply. This is to be expected because there is variability in the thickness of the trabecular meshwork, the extent of which is not known when ELT is performed. Additionally, the amount of pressure applied to the TM by the ELT delivery tip can also influence depth of treatment. Despite this discrepancy in the depth of treatment, much like the present report regarding FLT, ELT does not cause thermal collateral damage to the surrounding tissues. Berlin et al.[17] reported the patency of clear holes into the Schlemm's canal at 2.5 years after

ELT. This indicates little to no wound healing response or scar tissue formation, likely because of the lack of thermal collateral damage. Considering this, we expect a similar patency of FLT channels given the lack of thermal damage to the target and surrounding tissues.

Overall, the ViaLase laser system can create clear channels through the trabecular meshwork and into the Schlemm's canal through the intact cornea in a noninvasive, clinically applicable manner, with no thermal collateral damage to the surrounding tissue. The treatment results in significant IOP reduction in perfused cadaver eyes with little to no thermal collateral damage to surrounding tissue. This study supports the potential of the ViaLase, Inc., laser to provide a clinically applicable, noninvasive femtosecond laser treatment for glaucoma.

Acknowledgments

The authors thank the entire ViaLase, Inc. team for their tireless work and contributions.

Supported by Vialase, Inc., NIH EY030304, and Research to Prevent Blindness (RPB 203478).

Disclosure: **E.R. Mikula**, ViaLase, Inc. (E, P); **F. Raksi**, ViaLase, Inc. (E, P); **I.I. Ahmed**, ViaLase, Inc. (C); **M. Sharma**, ViaLase, Inc. (E); **G. Holland,** ViaLase, Inc. (E); **R. Khazaeinezhad,** ViaLase, Inc. (E); **S. Bradford** (N); **J.V. Jester** (N); **T. Juhasz,** ViaLase, Inc. (E, P)

References

1. Weinreb RN, Aung T, Medeiros FA. The pathophysiology and treatment of glaucoma: a review. *JAMA*. 2014;311:1901–1911.
2. Lusthaus J, Goldberg I. Current management of glaucoma. *Med J Aust*. 2019;210:180–187.
3. Newman-Casey PA, Robin AL, Blachley T, et al. The most common barriers to glaucoma medication adherence: a cross-sectional survey. *Ophthalmology*. 2015;122:1308–1316.
4. Leahy KE, White AJ. Selective laser trabeculoplasty: current perspectives. *Clin Ophthalmol*. 2015;9:833–841.
5. Garg A, Gazzard G. Selective laser trabeculoplasty: past, present, and future. *Eye (Lond)*. 2018;32:863–876.
6. Saheb H, Ahmed II. Micro-invasive glaucoma surgery: current perspectives and future directions. *Curr Opin Ophthalmol*. 2012;23:96–104.
7. Mendrinos E, Mermoud A, Shaarawy T. Nonpenetrating glaucoma surgery. *Surv Ophthalmol*. 2008;53:592–630.
8. Schlunck G, Meyer-ter-Vehn T, Klink T, Grehn F. Conjunctival fibrosis following filtering glaucoma surgery. *Exp Eye Res*. 2016;142:76–82.
9. Latina MA, Gulati V. Selective laser trabeculoplasty: stimulating the meshwork to mend its ways. *Int Ophthalmol Clin*. 2004;44:93–103.
10. Kagan DB, Gorfinkel NS, Hutnik CM. Mechanisms of selective laser trabeculoplasty: a review. *Clin Exp Ophthalmol*. 2014;42:675–681.
11. Ahmed IIK. MIGS and the FDA: what's in a name? *Ophthalmology*. 2015;122:1737–1739.
12. Samuelson TW, Katz LJ, Wells JM, Duh YJ, Giamporcaro JE. Randomized evaluation of the trabecular micro-bypass stent with phacoemulsification in patients with glaucoma and cataract. *Ophthalmology*. 2011;118:459–467.
13. Camras LJ, Yuan F, Fan S, et al. A novel Schlemm's canal scaffold increases outflow facility in a human anterior segment perfusion model. *Invest Ophthalmol Vis Sci*. 2012;53:6115–6121.
14. Minckler DS, Baerveldt G, Alfaro MR, Francis BA. Clinical results with the Trabectome for treatment of open-angle glaucoma. *Ophthalmology*. 2005;112:962–967.
15. Greenwood MD, Seibold LK, Radcliffe NM, et al. Goniotomy with a single-use dual blade: short-term results. *J Cataract Refract Surg*. 2017;43:1197–1201.
16. Durr GM, Toteberg-Harms M, Lewis R, Fea A, Marolo P, Ahmed IIK. Current review of excimer laser trabeculostomy. *Eye Vis (Lond)*. 2020;7:24.
17. Berlin MST-HM, Kim E, Vuong I, Giers U. Excimer laser trabeculostomy (ELT): an effective MIGS procedure for open-angle glaucoma. In: Samples JRA, I I K, ed. *Surgical innovations in glaucoma*. New York: Springer Science + Business Media, 2014:85–95.
18. Mikula E, Holland G, Srass H, Suarez C, Jester JV, Juhasz T. Intraocular pressure reduction by femtosecond laser created trabecular channels in perfused human anterior segments. *Transl Vis Sci Technol*. 2021;10:22.
19. Johnson DH, Tschumper RC. Human trabecular meshwork organ culture. A new method. *Invest Ophthalmol Vis Sci*. 1987;28:945–953.

20. Johnson DH, Tschumper RC. The effect of organ culture on human trabecular meshwork. *Exp Eye Res*. 1989;49:113–127.
21. Clark AF, Wilson K, de Kater AW, Allingham RR, McCartney MD. Dexamethasone-induced ocular hypertension in perfusion-cultured human eyes. *Invest Ophthalmol Vis Sci*. 1995;36:478–489.
22. Bahler CK, Hann CR, Fjield T, Haffner D, Heitzmann H, Fautsch MP. Second-generation trabecular meshwork bypass stent (iStent inject) increases outflow facility in cultured human anterior segments. *Am J Ophthalmol*. 2012;153:1206–1213.
23. Gulati V, Fan S, Hays CL, Samuelson TW, Ahmed II, Toris CB. A novel 8-mm Schlemm's canal scaffold reduces outflow resistance in a human anterior segment perfusion model. *Invest Ophthalmol Vis Sci*. 2013;54:1698–1704.
24. Hays CL, Gulati V, Fan S, Samuelson TW, Ahmed II, Toris CB. Improvement in outflow facility by two novel microinvasive glaucoma surgery implants. *Invest Ophthalmol Vis Sci*. 2014;55:1893–1900.
25. Wang YX, Xu L, Wei WB, Jonas JB. Intraocular pressure and its normal range adjusted for ocular and systemic parameters. The Beijing Eye Study. 2011. *PLoS One*. 2018;13:e0196926.
26. Phelps CD, Armaly MF. Measurement of episcleral venous pressure. *Am J Ophthalmol*. 1978;85:35–42.
27. Sit AJ, Ekdawi NS, Malihi M, McLaren JW. A novel method for computerized measurement of episcleral venous pressure in humans. *Exp Eye Res*. 2011;92:537–544.
28. Sit AJ, McLaren JW. Measurement of episcleral venous pressure. *Exp Eye Res*. 2011;93:291–298.
29. Toyran S, Liu Y, Singha S, et al. Femtosecond laser photodisruption of human trabecular meshwork: an in vitro study. *Exp Eye Res*. 2005;81:298–305.
30. Liu Y, Nakamura H, Witt TE, Edward DP, Gordon RJ. Femtosecond laser photodisruption of porcine anterior chamber angle: an ex vivo study. *Ophthalmic Surg Lasers Imaging*. 2008;39:485–490.
31. Nakamura H, Liu Y, Witt TE, Gordon RJ, Edward DP. Femtosecond laser photodisruption of primate trabecular meshwork: an ex vivo study. *Invest Ophthalmol Vis Sci*. 2009;50:1198–1204.
32. Chai D, Chaudhary G, Mikula E, Sun H, Kurtz R, Juhasz T. In vivo femtosecond laser subsurface scleral treatment in rabbit eyes. *Lasers Surg Med*. 2010;42:647–651.
33. Liao CS, Zhuo ZY, Yu JY, et al. Decrimping: the first stage of collagen thermal denaturation unraveled by in situ second-harmonic-generation imaging. *Appl Phys Lett*. 2011;98(15):153703.
34. Sun Y, Chen W-L, Lin S-J, et al. Investigating Mechanisms of Collagen Thermal Denaturation by High Resolution Second-Harmonic Generation Imaging. *Biophysical Journal*. 2006;91:2620–2625.
35. Seibold LK, Soohoo JR, Ammar DA, Kahook MY. Preclinical investigation of ab interno trabeculectomy using a novel dual-blade device. *Am J Ophthalmol*. 2013;155:524–529.e522.
36. Yu XB, Miller J, Yu PK, et al. Ablation of intraocular tissue with fiber-optic probe-delivered 266-nm and 213-nm laser energy. *Invest Ophthalmol Vis Sci*. 2009;50:3729–3736.